Available online at www.sciencedirect.com
SCIENCE DIRECT
Materials Research Bulletin 41 (2006) 1487–1495
Materials Research Bulletin
www.elsevier.com/locate/matresbu

The effect of addition of alcohol and calcination methods on the synthesis of layered $Li[Li_{1/5}Ni_{1/10}Co_{1/5}Mn_{1/2}]O_2$ using solid-state reaction method

Chi Hoon Song [a], A. Manuel Stephan [a,1], Soo Kyung Jeong [a], Ae Rhan Kim [a], Kee Suk Nahm [a,*], Yun Sung Lee [b], Jae Kook Kim [c], Hoon Taek Chung [d]

[a] School of Chemical Engineering & Technology, Chonbuk National University, Jeonju 561-756, Republic of Korea
[b] Faculty of Applied Chemical Engineering, Chonnam University, Kwangju 500-757, Republic of Korea
[c] Department of Materials Science & Engineering, Chonnam University, Kwangju 500-757, Republic of Korea
[d] Department of Ceramic Engineering, Dong-Shin University, 252 Naju, Chonnam 520-714, South Korea

Received 29 August 2005; received in revised form 18 January 2006; accepted 23 January 2006
Available online 20 February 2006

Abstract

$Li[Li_{1/5}Ni_{1/10}Co_{1/5}Mn_{1/2}]O_2$ solid solutions were prepared by four different routes using a solid-state reaction method. All the prepared samples were of a layered manganese oxide structure. The prepared samples were subjected to XRD, Raman and charge–discharge studies. The addition of ethyl alcohol in the starting materials during the synthesis process has exhibited superior electro-chemical properties and offered higher discharge capacity than the samples calcinated in the form of pellets without solvent. The added ethyl alcohol not only assists to get a homogeneous mixing of reacting species, but also influences the chemical reaction during the synthesis process. The materials are found to be superior in terms of minimum capacity fading per cycle than the materials so far reported. The other electro-chemical properties like irreversible capacity and discharge capacity of the synthesized materials have also been discussed based on the experimental observations.

Keywords: Layered compound; X-ray diffraction; Raman spectroscopy; Electro-chemical properties; High discharge capacity

1. Introduction

Recently, solid solutions of layered manganese oxides have been identified as promising cathode materials for lithium secondary batteries because they showed good structural stability and excellent electro-chemical properties [1–10]. Solid solutions with layered manganese oxides can be prepared either by a sol–gel [11–16] or by a solid-state reaction method [17,18]. But most of the solid solutions are synthesized using a sol–gel method because it provides a homogeneous mixing of starting materials, a high reactivity of the mixture even at a lower heating treatment and at a shorter reaction time. This homogeneous mixing results in an easier control of the stoichiometric synthesis of the

* Corresponding author. Tel.: +82 63 270 2311; fax: +82 63 270 2306.
E-mail address: nahmks@chonbuk.ac.kr (K.S. Nahm).
[1] On deputation from: Central Electrochemical Research Institute, Karaikudi 630 006, India.

0025-5408/$ – see front matter
doi:10.1016/j.materresbull.2006.01.031

materials at an atomic level. For commercialization, however, the solid-state reaction method has been mainly employed for the preparation of cathode materials since the former is a more expensive process than the latter.

Poor solid-phase diffusivity of the chemical species during the synthesis process generally causes the formation of material with unstable structures, resulting in poor electro-chemical behaviors [19,20]. In order to circumvent these drawbacks, many researchers switched over to other alternative processes, such as calcination of starting materials at high temperature, calcinations of materials in the form of pellets or/and addition solvents during the synthesis process [21–23]. But high temperature synthesis frequently causes the sublimation of the Li ion from lithium metal oxides, whereas pellet-shaped calcination process needs a longer synthesis time. Spinel $LiMn_2O_4$ was synthesized by grinding MnO_2 and LiOH starting materials with alcohol as a dispersing agent to obtain high material utilization and to extend cycleability at high rates. The spinel showed a limited discharge capacity fading even at 6 mA/cm^2 (520 mAh/g) [21]. It was reported that the (low temperature) LT α-$LiFeO_2$ could be synthesized at a low temperature route via the H^+/Li^+ ionic exchange reaction in LiOH–H_2O/α-FeOOH/alcohol system with a high water concentration and the disordered rock-salt LT α-$LiFeO_2$ was subjected to cycling studies with a cycling capacity of ca. 0.2Li/$LiFeO_2$ [23]. Although some studies were made on the solid-state synthesis of lithium metal oxides ($LiFeO_2$, $LiFePO_4$, etc.) using alcohol and its derivative as a reaction medium [22,23], not much studies have been reported on the synthesis of lithium manganese oxides using alcohol as a solvent. Moreover, the effect of addition of solvent during the synthesis process was not studied for the layered manganese oxides solid solutions. Moreover, it is not clearly understood how alcohol (or/and alcohol derivatives) affects the structural and electro-chemical properties of the synthesized materials.

In the present study, $Li[Li_{1/5}Ni_{1/10}Co_{1/5}Mn_{1/2}]O_2$ solid solution composition was synthesized by solid-state method with various synthesis processes. We employed four synthetic routes; with and without addition of alcohols in the precursors, and powder- and pellet-shaped calcination of precursors. We examined the effect of addition of the alcohol, and the form of the starting materials, pellet or powder during the synthesis process on the structural and electro-chemical properties of the synthesized solid solutions. The influence of alcohol on the structural and electro-chemical properties of the layered $Li[Li_{1/5}Ni_{1/10}Co_{1/5}Mn_{1/2}]O_2$ solid solution is presented.

2. Experiment

Stoichiometric amounts of lithium, nickel, cobalt, and manganese hydroxides (LiOH, $Ni(OH)_2$, MnOOH, and $Co(OH)_2$) were mixed with a cation ratio of Li:Ni:Co:Mn = 6/5:1/10:1/5:1/2 for the preparation of $Li[Li_{1/5}Ni_{1/10}Co_{1/5}Mn_{1/2}]O_2$. The mixture of the starting materials was ground using a ball miller (FRITSCH; Planetary Mono Mill-Pulverisette 6). The ground mixture was calcined using two different processes. Table 1 depicts the sample name and their method of preparation. The first process involved the calcination of the mixture in the form of a powder. The ground mixture was pre-calcined at 600 °C for 10 h. The pre-calcined powders were ground with the ball miller and calcined again at 940 °C for 10 h. This synthesized sample was named as sample A. The second process involved the calcination of the mixture in the form of a disc-shaped pellet. The ground mixture was pressed at 400 kg cm^{-2} to form a disc-shaped pellet and the pellet was heated at 600 °C for 10 h. The pre-calcined sample was ground and was pressed to make the disc-shaped pellet again. The pellet was calcined at 940 °C in air for 10 h. The prepared sample was named sample B. The grinding time was 4 h for all the processes, and the calcinations were performed in air. To study the effect of ethyl alcohol on the mixing of solid-phase starting materials, the same stoichiometric amounts of the materials were mixed in the presence of ethyl alcohol (0.5 cc/g of solid), and the mixture was ground using a ball miller. To evaporate ethyl alcohol, the ground mixture was heated at 70–80 °C for 10 h in air. The same procedure was employed for the preparation of $Li[Li_{1/5}Ni_{1/10}Co_{1/5}Mn_{1/2}]O_2$ without ethyl alcohol. The structure of the prepared samples was characterized using X-ray diffraction (XRD, D/Max-3A, Rigaku) with a Cu Kα radiation. XRD measurements were

Table 1
Sample names and their preparation method

Sample	Preparation method of the sample
A	Powder without alcohol
B	Pellet without alcohol
C	Powder with alcohol
D	Pellet with alcohol

carried out in the 2θ range of 10–80° with a scan speed of 4°/min. In order to avoid the loss of lithium due to evaporation, an excess of lithium up to 10% was added. The Li, Co, Mn, Ni contents in the resulting materials was analyzed using an inductively coupled plasma/atomic emission spectrometer (ICP/AES, Kontron-S 35). Energy Dispersive X-ray spectrometer (EDX: EMAX, HOBRIBA) measurements were carried out to analyze the chemical composition of the synthesized materials.

The electro-chemical characterization was carried out using CR2032 coin-type cells. The detailed description of the cell fabrication was reported elsewhere [4,5]. The charge and discharge processes were carried out at a current density of 0.4 mA/cm^2 (20 mA/g) with cut-off voltages between 2.5 and 4.5 V (versus Li/Li$^+$).

3. Results and discussion

Fig. 1(a)–(d) show the XRD patterns with their corresponding Miller indices for the samples A, B, C, and D, respectively. All samples are indexed as a layered manganese oxide structure based on a hexagonal α-$NaFeO_2$ structure (space group: R3_m, 166) [24], except the superlattice ordering peaks between 20° and 25°. The impurity peaks are resulted from the short range ordering of Li, Co, Ni and Mn atoms in the transition metal layers [24,25], indicating the characteristic feature of Li_2MnO_3 structure [1,24,25]. The characteristic XRD peaks of the hexagonal structure apparently appear at 2θ = 18, 37, 38, 38.5, 45, 64.5, and 65.5 for 0 0 3, 1 0 1, 0 0 6, 0 1 2, 1 0 4, 0 1 8, and 1 1 0 planes, respectively. The intensity ratios of (0 0 3)/(1 0 4) peaks for all samples are above 1.38. According to Morales et al. [26] who reported that the (0 0 3) peak occurs from the diffraction of the layered rock-salt structure ($R\bar{3}m$), whereas the (1 0 4) peak appears from both the diffractions of layered as well as cubic rock-salt structures. It has been observed that layered cathode materials produce good electro-chemical properties when the intensity ratio of (0 0 3) and (1 0 4) peaks is higher than 1.2, and the (1 0 1), (0 0 6) peaks and (1 0 8), (1 1 0) peaks are clearly split. The above structural characterization clearly substantiates that all the samples are synthesized with a typical layered structure.

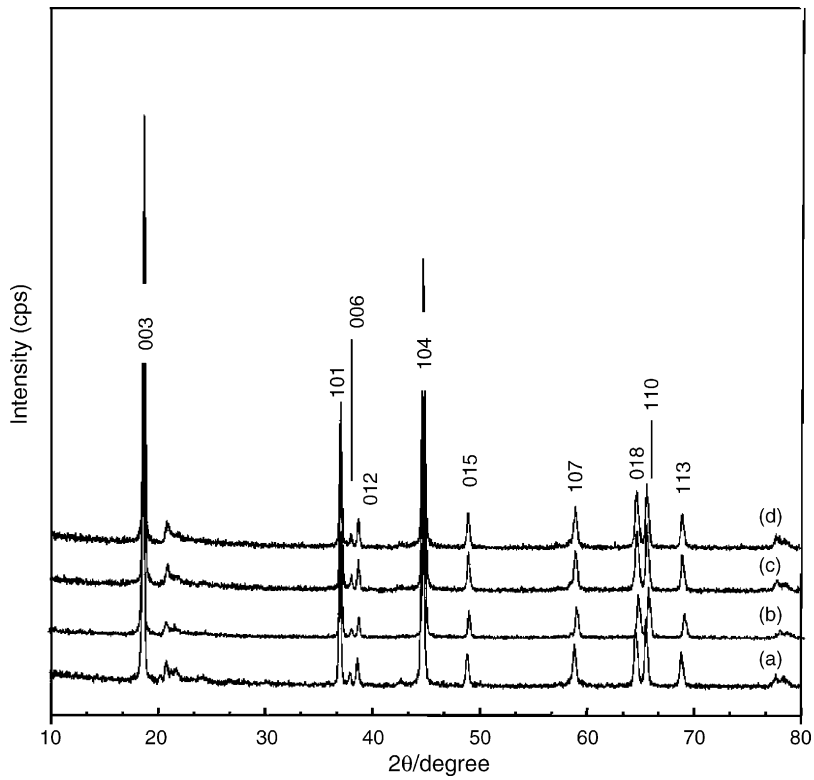

Fig. 1. X-ray patterns of $Li[Li_{1/5}Ni_{1/10}Co_{1/5}Mn_{1/2}]O_2$ materials prepared for the samples (a), (b), (c) and (d).

The chemical composition of the samples synthesized by four different synthetic processes was measured by EDX measurements. The moles of constitute elements were measured from EDX data of the samples and were divided by the moles of Ni to calculate the molar ratios of each chemical species. The molar ratios of each species for the samples were compared with those of theoretically calculated from the stoichiometric composition of the sample. Although not shown in this paper, the measured molar ratios of each species for the samples were in accordance with the theoretically calculated values, indicating that our samples were synthesized with good stoichiometry. The ICP-AES studies reveal that the samples A, B, C and D have the composition of $Li_{1.18}Ni_{0.1}Co_{0.2}Mn_{0.5}O_2$, $Li_{1.19}Ni_{0.1}Co_{0.2}Mn_{0.5}O_2$, $Li_{1.20}Ni_{0.1}Co_{0.2}Mn_{0.5}O_2$ and $Li_{1.22}Ni_{0.1}Co_{0.2}Mn_{0.5}O_2$, respectively.

The discharge capacities versus voltage profile of the samples A, B, C and D at room temperature are shown in Fig. 2(a)–(d), respectively. All the samples show a monotonic discharge curve, although their electro-chemical performances are different. This is a characteristic feature of typical layered manganese oxides solid solutions. For example the sample A shows a charging capacity of 153 mAh/g and a discharge capacity of 107 mAh/g with an irreversible capacity loss of about 46 mAh/g. Similarly the samples B, C and D, respectively, shows an irreversible capacity loss of 60, 85 and 96 mAh/g during their first charge–discharge cycle. (This irreversible capacity loss is shown as a square box in Fig. 2.) According to Lu and Dahn [25], who clearly demonstrated with in situ XRD for $Li[Ni_xLi_{(1/3-2x/3)}Mn_{2/3-x/3}]O_2$, the appearance of this plateau region is attributed to the irreversible loss of oxygen. Another possibility for the charge compensation at voltage higher than 4.5 V is participation of oxygen ions in the redox reaction. A similar observation was reported by Kang et al. [13] for the $Li(Li_{0.2}Ni_{0.2}Mn_{0.6})O_2$ system. Fig. 3 shows the discharge capacities of the samples measured at room temperature as a function of the cycle number. The samples A, B, C, and D deliver the initial discharge capacities of 107, 116, 147, and 146 mAh/g, respectively. Upon 50 cycles the discharge capacities of the samples were found to be 139, 150, 174, and 185 mAh/g for the samples A, B, C and D, respectively. These values are much lower than the capacity of the material (231 mAh/g) synthesized by a sol–gel method [4], but are comparable or superior to those of so far reported cathode materials synthesized by a solid-state synthesis [17,18]. The discharge capacities of the samples are summarized in a table in Fig. 3, together with their retention ratios.

It is interesting to note that the discharge capacities of the samples prepared with ethyl alcohol (samples C and D) are much higher than those of the samples prepared without ethyl alcohol (samples A and B). But the samples

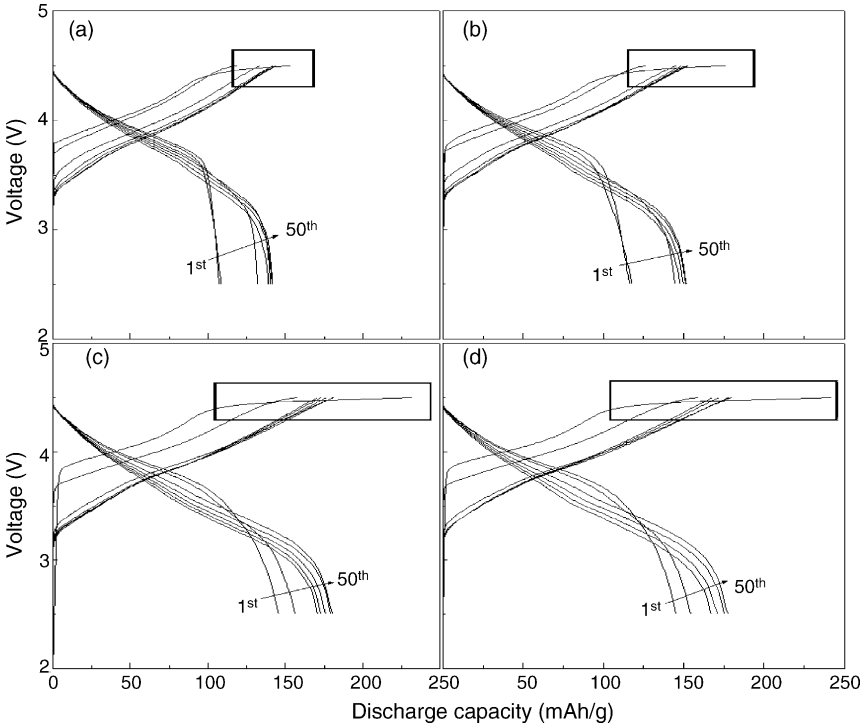

Fig. 2. Voltage vs. capacity for $Li[Li_{1/5}Ni_{1/10}Co_{1/5}Mn_{1/2}]O_2$ materials prepared in the forms of (a) powder, (b) pellet form, (c) powder with ethyl alcohol and (d) pellet form with ethyl alcohol. The first and fiftieth cycles are indicated. Rectangle box indicates the irreversible capacity region.

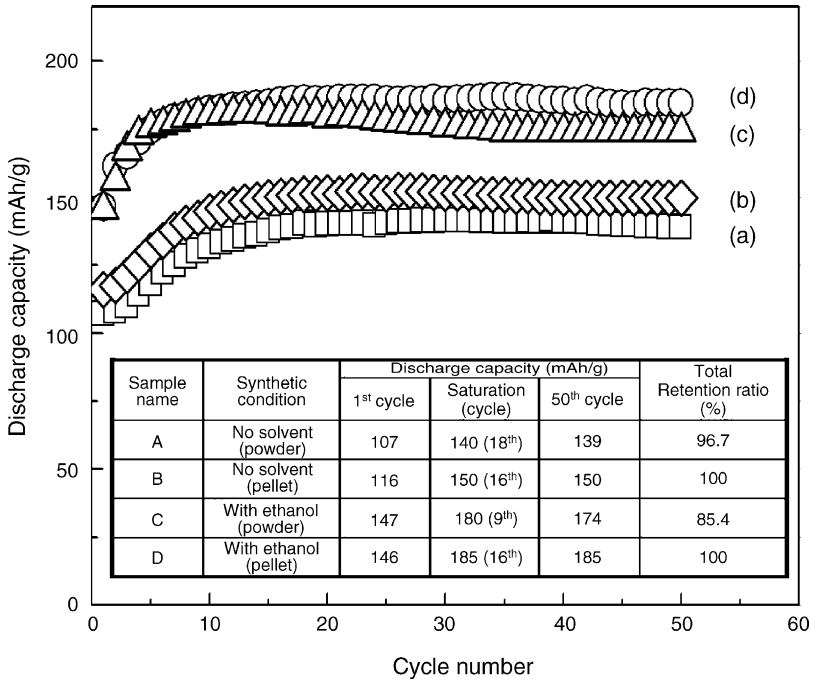

Sample name	Synthetic condition	Discharge capacity (mAh/g)			Total Retention ratio (%)
		1st cycle	Saturation (cycle)	50th cycle	
A	No solvent (powder)	107	140 (18th)	139	96.7
B	No solvent (pellet)	116	150 (16th)	150	100
C	With ethanol (powder)	147	180 (9th)	174	85.4
D	With ethanol (pellet)	146	185 (16th)	185	100

Fig. 3. Discharge capacity vs. cycle number for $Li[Li_{1/5}Ni_{1/10}Co_{1/5}Mn_{1/2}]O_2$ materials prepared in the forms of powder (a) powder, (b) pellet form, (c) powder with ethyl alcohol and (d) pellet form with ethyl alcohol.

synthesized in the form of pellets (samples B and D) show slightly higher discharge capacities than the samples prepared in the un-pelletized form.

The effect of alcohol in the mixing of solid-phase precursors was reported on the solid-state reaction synthesis of other cathode materials, such as $LiFeO_2$, spinel $LiMn_2O_4$, etc. [21–23,27]. It was suggested that the use of various alcohols enhances the homogeneous mixing of solid precursors, resulting in the synthesis of better crystallographic structures. But the exact synthesis mechanism of the solid-state reaction system has not yet been proposed. Meanwhile, it was generally reported that pressing method enhances solid-phase diffusion of precursor components during calcinations, leading to better crystallographic ordering [22,23]. But for the palletized samples B and D no discernible changes could be observed from our experiments.

It is evident, that the use of ethyl alcohol is very effective in obtaining a higher discharge capacity than the calcinations method in the solid-state synthesis. It suggests that ethyl alcohol functions as a good medium to successfully synthesize $Li[Li_{1/5}Ni_{1/10}Co_{1/5}Mn_{1/2}]O_2$ solid solution by a solid-state reaction. In solid-state reaction synthesis in the absence of alcohol, solid-phase diffusion generally occurs by the mechanical mixing and thermal effect. Therefore, the diffusion rates of the solid reacting species may be slow. The poor solid-phase diffusivities of the reacting species generally cause the formation of unstable structured materials, resulting in poor electrochemical behaviors. Synthesizing the samples with the addition of solvents during the ball mill mixing, on the other hand, seems that the added solvent not only enhances the homogeneous mixing of reacting species, but also facilitates the chemical reaction during the synthesis. Our ICP-AES analysis also supports this phenomena i.e., the samples prepared with the addition of alcohol and pelletized were found have better stoichiometry with higher lithium ion content.

To understand the abrupt increase of the discharge capacity of the samples C and D synthesized in the presence of ethyl alcohol, the chemistry of alcohol and starting materials was studied. The preparation of $Li[Li_{1/5}Ni_{1/10}Co_{1/5}Mn_{1/2}]O_2$ solid solution was performed with corresponding metal hydroxides in the presence of ethyl alcohol. In the presence of ethyl alcohol, lithium hydroxide reacts with the alcohol, which forms lithium alkoxide (LiOR), as written in the following equation:

$$Li^+OH^{-\bullet}xH_2O + RO^-\text{-}H^+ \leftrightarrow Li^+OR^- + xH_2O \quad (R : CH_3CH_2^-). \tag{1}$$

LiOH dissociates into Li^+ and OH^- and, similarly, ethyl alcohol decomposes into RO^- ($CH_3CH_2O^-$) and H^+. During the reaction, a negatively charged RO^- will combine with a positively charged Li^+ ion and forms LiOR. Accordingly, the OH^- ion will combine with H^+ ion to form water molecules. However, this reaction is reversible. Forward reaction is much more favorable than the reverse reaction, because LiOH is a stronger base than LiOR. The LiOR formed in reaction (1) participates in the reaction with $Ni(OH)_2$, $Co(OH)_2$, and MnOOH to form $Li[Li_{1/5}Ni_{1/10}Co_{1/5}Mn_{1/2}]O_2$ in the following equation:

$$5/6\text{LiOR} + 1/10\text{Ni(OH)}_2 + 1/5\text{Co(OH)}_2 + 1/2\text{MnOOH} \rightarrow \text{Li}[\text{Li}_{1/5}\text{Ni}_{1/10}\text{Co}_{1/5}\text{Mn}_{1/2}]\text{O}_2 + 5/6\text{R-OH} + x\text{H}_2\text{O}. \quad (2)$$

This suggests that the added ethyl alcohol in the mixing process participates not only in the chemical reaction during the synthesis, but also apart from enhances the diffusivity of the chemical species. However, these effects are not observed in the synthesis of the samples without the addition of alcohol, which results in poor electro-chemical behaviors.

More interestingly this is observed from Fig. 3 that the discharge capacities of all the samples initially increased with cycling to saturation at maximum discharge capacities, although the discharge capacities of the samples are different. The electro-chemical behavior, which shows an increase of discharge capacity at initial cycle numbers, was frequently observed in layered manganese oxide solid solutions with a Li ion in their transition metal layers [1,6,11,14,24] and is attributed to the stabilization of synthesized solid solutions with cycling [1] or due to the change of Mn oxidation state from 4+ to 3+ (during discharge process) or from 3+ to 4+ (during charge process) during cycling [3], or due to the contribution of lithium ions removed from transition metal layers while cycling [4,14,15]. However, the increase of capacity upon cycling has not yet been clearly understood. Hence, it appears that as a general consensus these materials have extremely complex structures.

Kim and Sun [11] explained that the fast rates of the Li ion insertion/extraction gradually stabilize the structure of manganese oxides with cycling, resulting in the increase of discharge capacity at initial cycles. The increase of the initial discharge capacity is also explained by the contribution of Mn [4,5,11,13,14]. Yoon et al. [28] demonstrated by X-ray absorption spectroscopy that the Mn ions in the pristine samples are already in the Mn^{4+} oxidation state and are not oxidized as a result of the Li-deintercalation; however, the average oxidation state of Ni increases during the charge.

It is noted that all the samples produce the irreversible capacity at the first charging cycle (shown with an inset rectangular box in Fig. 2), although the magnitudes of the capacities are different. The irreversible capacities of samples C (86 mAh/g) and D (97 mAh/g) synthesized in the presence of ethyl alcohol are longer than those of samples A (47 mAh/g) and B (60 mAh/g) synthesized without the alcohol. The values of the irreversible capacities of the samples decreased in the order of sample D > sample C > sample B > sample A. The origin of the irreversible capacity is still unclear. It is reported that the irreversible capacity results from oxygen loss in the structure [1,4,5] or extraction of the Li ion from transition metal layers [13]. It is observed that the cathode materials, which produce the irreversible capacity, increase the discharge capacity at the initial cycle numbers. Higher discharge capacity is generally attained from the materials [29] and the saturation capacities of these materials increase in proportion to the magnitude of the irreversible capacity [17,29].

The lattice parameters, *a* and *c*, were calculated using Rietveld refinement for XRD data of all samples and are shown in Fig. 4. It is seen that the lattice parameters *a* and *c* for samples A and B are smaller than those of samples C and D. The values of the lattice parameters (*a* and *c*) of the samples decrease in the order of sample D > sample C > sample B > sample A. The *a* and *c* axes increase with the increased Li ion content in the transition metal layers, because the radius of Li^+ ion ($\gamma = 0.76$ Å) is bigger that that of Ni^{2+} ($\gamma = 0.69$ Å), Co^{3+} ($\gamma = 0.545$ Å), Mn^{4+} ($\gamma = 0.53$ Å) 12. This implies that the Li ion content in the transition metal layers of $Li[Li_{1/5}Ni_{1/10}Co_{1/5}Mn_{1/2}]O_2$ solid solution increases in the order of sample D > sample C > sample B > sample A. The values of *a* and *c* for $Li[Li_{1/5}Ni_{1/10}Co_{1/5}Mn_{1/2}]O_2$ synthesized using a sol–gel method were 2.8477 and 14.2282, respectively [4]. This indicates that the stoichiometry of the samples was obtained in the presence of ethyl alcohol by the increased substitution of Li ions in the transition metal sites. Consequently, it is considered that ethyl alcohol added in the mixing process of solid-phase starting materials enhances the solid diffusivity and chemical reaction rate in the solid-state synthesis to form a favorable structure of $Li[Li_{1/5}Ni_{1/10}Co_{1/5}Mn_{1/2}]O_2$ solid solution with increased Li ion content in the transition metal layer.

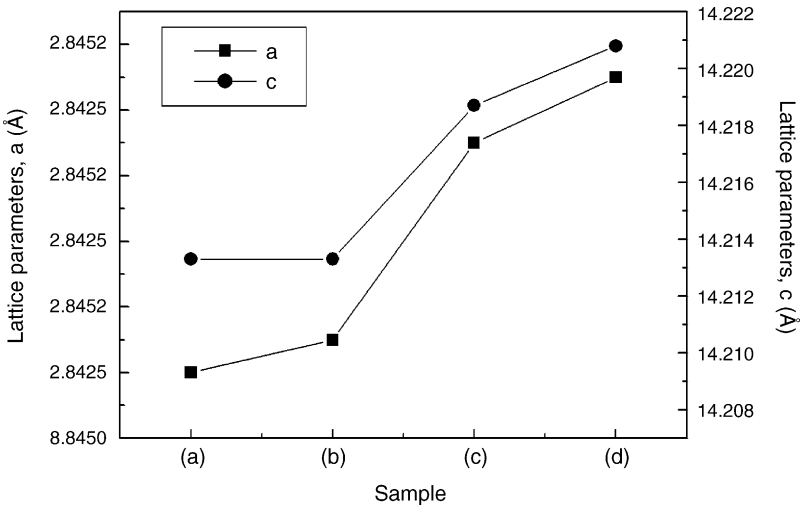

Fig. 4. The plot of the lattice constants, a and c, vs. type of the synthesized samples.

Fig. 5 shows the plot of dQ/dV curves versus voltage in the range of 2.5–4.5 V for sample D. For other samples, although not presented in this paper, the dQ/dV curves were almost similar in shape. In the charge process, the peaks observed between 3.7 and 4.1 V are due to the oxidation of Ni^{2+} to Ni^{4+} in the material. The oxidation peak of Mn^{3+} to Mn^{4+} rises and ends 3.5 V, which is not observed at the first charge process in any of the samples. The drastically increased oxidation peak above 4.46 V is due to the irreversible capacity, corresponding to the irreversible plateau in the first cycle as shown in Fig. 2. The corresponding reduction peaks of Ni^{4+} to Ni^{2+} and Mn^{4+} to Mn^{3+} appear in the discharge process around 3.7 and 3.3 V, respectively. In the first charge process, the oxidation peak from Mn^{3+} to Mn^{4+} is not generated from all the samples. This indicates that the as-prepared samples were synthesized with maintaining

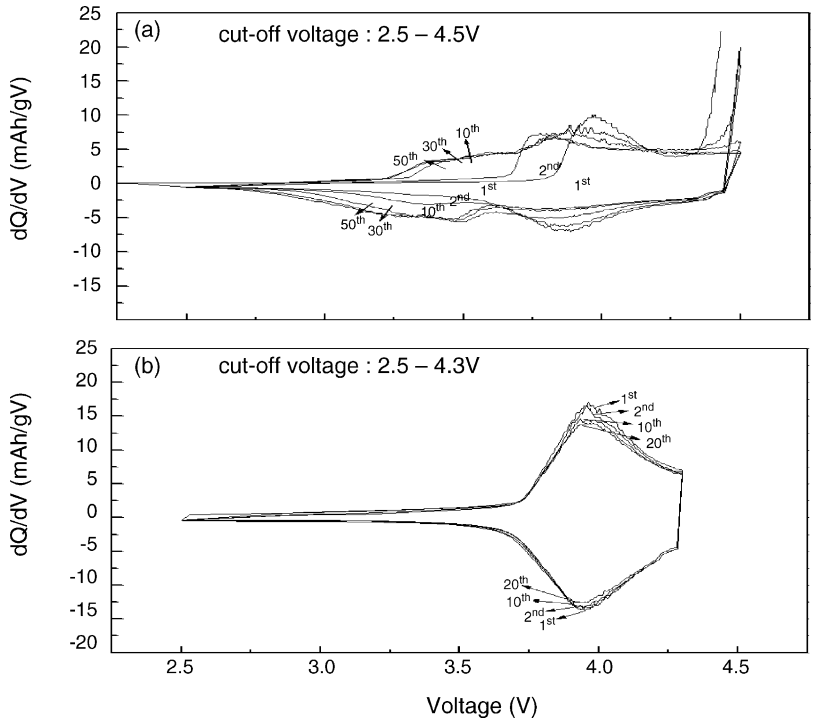

Fig. 5. Differential capacity vs. potential for $Li[Li_{1/5}Ni_{1/10}Co_{1/5}Mn_{1/2}]O_2$ materials prepared in the forms of pellet with ethyl alcohol. (a) Cut-off voltage: 2.5–4.5 V, (b) cut-off voltage: 2.5–4.3 V. First to fiftieth cycles are indicated.

the oxidation state of 4+. The peak begins to appear, however, from the second charge process in the as-prepared samples. Another typical characteristic in the shape of the dQ/dV curves of the samples is that the irreversible peak occurs above 4.46 V in all the samples. The irreversible peaks for samples C and D are higher in the amplitude than those of samples A and B. In addition, samples C and D show the irreversible peak even after more cycles, although the peak decreases with cycle number. This electro-chemical behavior results in a continuous capacity increase with cycle number with the delivery of higher capacity, as observed by many researchers [1,4–6,13].

The oxidation/reduction of the Mn ion peaks is also observed below 3.5 V in samples A, B, C, and D during charge/discharge cycles. This means that the growth of Mn^{3+}/Mn^{4+} coupled peaks is closely related to the gradual increase of the discharge capacity during initial cycles. There are some discussions on the relationship of irreversible capacity, increased initial capacity, and high capacity in the literature [4–6,11,13,14]. During the first charge, Li ions were removed from the lithium layer and, simultaneously, Ni^{2+} is oxidized to Ni^{4+} upon charge to 4.45 V. Further charging above 4.5 V brings about oxygen loss and Li ion extraction from the transition metal layers. The extraction of the Li ion from the transition metal layers induces a change in the oxidation state of the manganese in order to keep the electroneutrality, which results an increase in the capacity of the $Li[Li_{1/5}Ni_{1/10}Co_{1/5}Mn_{1/2}]O_2$ electrode. As shown in Fig. 4, which presents the saturation of discharge capacity curve after few cycling, the growth of the Mn oxidation peak levels off after a few cycles [4,5].

Further, in order to confirm our statement, that the increase of the discharge capacity is due to the change of the Mn oxidation state, we examined the dQ/dV curves versus voltage in the range of 2.5–4.3 V and are shown in Fig. 5(b). It is interesting to note that the peaks due to the irreversible capacity and the Mn^{3+}/Mn^{4+} couples are not detected in the measurements. The Ni^{2+}/Ni^{4+} couple peaks are only observed during the oxidation and reduction processes. This clearly demonstrates that there is a close relationship among irreversible capacity, increased initial capacity, and high capacity, and the change of the Mn oxidation state during the charge and discharge processes.

4. Conclusions

The $Li[Li_{1/5}Ni_{1/10}Co_{1/5}Mn_{1/2}]O_2$ solid solution was synthesized using a solid-state reaction with various synthesis processes. The structural and electro-chemical characterization was performed for the samples synthesized with and without ethyl alcohol during synthesis process. The samples were all synthesized with a typical layered structure with a good stoichiometry. The discharge capacities of the samples prepared with ethyl alcohol were much higher than that of the samples prepared without ethyl alcohol. The sample synthesized in the form of pellets makes no difference in terms of capacity with the samples prepared in the form of powders. It is quite obvious from our results that the use of ethyl alcohol is an effective way to obtain materials with higher discharge capacity. The irreversible capacity, the increased initial capacity, and the high discharge capacity were systematically correlated based on the experimental observations.

Acknowledgement

This work was supported by Ministry of Science and Technology, 2004.

Reference

[1] Z. Lu, J.R. Dahn, J. Electrochem. Soc. 149 (2002) A815–A822.
[2] K. Numata, C. Sakaki, S. Yamanaka, Solid State Ionics 117 (1999) 257–263.
[3] B. Ammundsen, J. Paulsen, Adv. Mater. 13 (2001) 943–956.
[4] K.S. Park, M.H. Cho, S.J. Jin, K.S. Nahm, Y.S. Hong, Solid State Ionics 171 (2004) 141–146.
[5] K.S. Park, M.H. Cho, S.J. Jin, K.S. Nahm, J. Electrochem. Solid State Lett. 7 (2004) A239–A241.
[6] Z. Lu, K.K. MacNeil, J.R. Dahn, J. Electrochem. Solid-State Lett. 4 (2001) A191–A194.
[7] R.D. Shannon, Acta Crystallogr. A 32 (1976) 751–767.
[8] S.-T. Myung, S. Komaba, N. Kumagai, J. Electrochem. Soc. 149 (2002) A1349–A1357.
[9] S. Jouanneau, K.W. Eberman, L.J. Krause, J.R. Kahn, J. Electrochem. Soc. 150 (2003) A1637–A1642.
[10] A.M. Kannan, A. Manthiram, J. Electrochem. Soc. 150 (2003) A349–A353.
[11] J.H. Kim, Y.K. Sun, J. Power Sources 119–121 (2003) A166–A170.
[12] Z. Lu, J.R. Dahn, J. Electrochem. Soc. 149 (2002) A1454–A1459.
[13] S.H. Kang, Y.K. Sun, K. Amine, Electrochem. Solid-State Lett. 6 (2003) A183–A186.

[14] S.H. Kang, K. Amine, J. Power Sources 124 (2003) 533–537.
[15] S. Jouanneau, D.D. Macneil, Z. Lu, S.D. Beattie, G. Murphy, J.R. Dahn, J. Electrochem. Soc. 150 (2003) A1299–A1304.
[16] S. Castro-Garcia, A. Castro-Couceiro, M.A. Seňarís-Rodrīguez, F. Soulette, C. Julien, Solid State Ionics 156 (2003) 15–26.
[17] L. Zhang, K. Takada, N. Ohta, L. Wang, T. Sasaki, M. Watanabe, Mater. Lett. 58 (2004) 3197–3200.
[18] Y.-K. Sun, S.-H. Kang, K. Amine, Mater. Res. Bull. 39 (2004) 819–825.
[19] M.N. Obrovac, O. Mao, J.R. Dahn, Solid State Ionics 112 (1998) 9–19.
[20] W.T. Jeong, K.S. Lee, J. Power Sources 104 (2002) 195–200.
[21] G. Pistoia, R. Rosati, J. Power Sources 58 (1996) 135–138.
[22] Y. Sakurai, H. Arai, S. Okada, J.I. Yamaki, J. Power Sources 68 (1997) 711–715.
[23] Y. Sakurai, H. Arai, J.-I. Yamaki, Solid State Ionics 113–115 (1998) 29–34.
[24] Z. Lu, L.Y. Beaulieu, R.A. Donaberger, C.L. Thomas, J.R. Dahn, J. Electrochem. Soc. 149 (2002) A778–A791.
[25] Z. Lu, J.R. Dahn, J. Electrochem. Soc. 150 (2003) A1044–A1051.
[26] J. Morales, C. Peres-Vicente, J.L. Tirado, Mater. Res. Bull. 25 (1990) 623–630.
[27] Y.S. Lee, S. Sato, Y.K. Sun, K. Kobayakawa, Y. Sato, Electrochem. Commun. 5 (2003) 359–364.
[28] W.S. Yoon, C.P. Grey, X.Q. Yang, D.A. Fischer, J. MaBreen Electrochem. Solid State Lett. 7 (2004) A53.
[29] Y.J. Park, Y.S. Hong, X. Wu, K. Sun Ryu, S.H. Chang, J. Power Sources 129 (2004) 288–295.